AJNR

Diffusional Kurtosis along the Corticospinal Tract in Adult Normal Pressure Hydrocephalus

B. Ades-Aron, S. Yeager, N. Miskin, E. Fieremans, A. George and J. Golomb

Diffusional Kurtosis along the Corticospinal Tract in Adult Normal Pressure Hydrocephalus

B. Ades-Aron, S. Yeager, N. Miskin, E. Fieremans, A. George, and J. Golomb

ABSTRACT

BACKGROUND AND PURPOSE: Normal Pressure Hydrocephalus is a reversible form of dementia characterized by enlarged ventricles, which can deform and cause disruptions to adjacent white matter fibers. The purpose of this work was to examine how diffusion and kurtosis parameters vary along the corticospinal tract and determine where along this path microstructure is compromised in patients diagnosed with normal pressure hydrocephalus. We hypothesized that disruption of the corticospinal tract from ventricular enlargement can be measured using diffusion MR imaging and this will be quantified in periventricular regions.

MATERIALS AND METHODS: We developed a method to analyze diffusion parameters at discrete points along neural tracts. We then used diffusion MR imaging data from patients with Alzheimer disease and healthy controls to compare whether diffusion along the corticospinal tract differs from that of patients with normal pressure hydrocephalus.

RESULTS: We found that diffusion parameters can differentiate patients with normal pressure hydrocephalus from those with Alzheimer disease and healthy controls: Axial diffusion, axial kurtosis, and the axonal water fraction were found to differ significantly across groups ($P < .05$) in an area located close to the superior internal capsule and corona radiata but below the cortex.

CONCLUSIONS: A lower axonal water fraction indicates a lower axonal density in the corticospinal tract, which may indicate permanent damage. Lower axial kurtosis may imply that axons are being more aligned due to compression.

ABBREVIATIONS: AD = axial diffusivity; AK = axial kurtosis; AUC = area under the receiver operating characteristic curve; AWF = axonal water fraction; CST = corticospinal tract; FA = fractional anisotropy; NPH = normal pressure hydrocephalus

The most widely accepted treatment for normal pressure hydrocephalus (NPH) symptoms is ventriculoperitoneal shunt placement, which can result in profound symptom amelioration, predominantly gait impairment.[1] Despite the well-established clinical features and the requisite cardinal radiologic feature of dilated ventricles, the mechanisms relating ventricular enlargement to clinical deficits and how fluid-dynamic alterations in CSF post-shunt placement lead to gait improvement are poorly understood.

Previous studies using structural or functional imaging have indicated that mechanical compression of corticospinal white matter due to ventricular enlargement is responsible for gait disturbances commonly associated with NPH.[2,3] Diffusional kurtosis imaging quantifies the contribution of non-Gaussian diffusion effects, such as the presence of microstructure in the brain.[4,5] The white matter tract integrity[6] model is a method that relates diffusional kurtosis imaging–compatible metrics to white matter microstructure by partitioning water into an intra-axonal compartment and an extra-axonal compartment and computing the axonal water fraction (AWF), which is sensitive to demyelination and axonal atrophy.[7-9] These biomarkers may be used to represent the pathology occurring at the mesoscopic scale.

The corticospinal tract (CST) is altered by mechanical deformation resulting from ventricular enlargement, and we hypothesized that this compression can be measured using a combination of diffusion MR imaging and tractography of the CST. Here, we examined how diffusion and kurtosis parameters vary along the corticospinal tract and determined where, along this path, micro-

Table 1: Key demographic information

	No. of Subjects	Age (Range) (Mean) (yr)	Male/Female Ratio
NPH	23	58–87 (76.9)	13:10
Alzheimer disease	10	56–81 (74.9)	5:5
Controls	11	60–87 (75)	6:5

structure is compromised in patients diagnosed with NPH. We localized pathology in NPH using an along-tract analysis of diffusion to determine whether this method can differentiate patients with NPH from those with Alzheimer disease and healthy controls and to study whether diffusion biomarkers can assess cell damage due to ventricular expansion. We studied patients with Alzheimer disease in addition to controls due to common radiologic features such as ventriculomegaly and the relatively common (31%–75%) comorbidity of the 2 diseases.[10] We further investigated the relationship between CST injury and the presence of leukoaraiosis in NPH. We expect that in NPH, CST disruption would be maximal in the periventricular regions deformed by the enlarged lateral ventricles and not at sites distant to these locations.

MATERIALS AND METHODS
Demographics and Clinical Data
This retrospective, anonymized, single-center study was approved by the institutional review board with a waiver of consent and was Health Insurance Portability and Accountability Act–compliant. Demographics of the 3 patient groups (total $n = 44$) are given in Table 1. The 3 groups did not statistically differ in demographic characteristics.

Patients with NPH were selected from a pool of patients with enlarged ventricles and gait impairment referred to the New York University Adult Hydrocephalus Evaluation Program and evaluated by a neurologist (J.G.) with 25 years of experience. These patients all exhibited a characteristic dyspraxic gait, variable degrees of cognitive impairment, and symptoms of overactive bladder. From the initial chart review of patients with NPH from January 2003 through December 2014 ($n = 624$), we selected patients who fulfilled the following requirements: 1) completed a high-volume lumbar puncture or lumbar drain that resulted in convincing clinical improvement (clinician [J.G.] and the family's subjective impression of gait improvement), ($n = 101$); 2) the availability of preoperative 3T MR imaging acquired locally, which included a high-resolution MPRAGE sequence as well as diffusion images appropriate for diffusional kurtosis imaging analysis ($n = 20$); and 3) free of comorbidities such as cerebrovascular disease, coexisting intracranial mass lesions, or prior craniectomy identified by a neuroradiologist (A.G.). The final sample size was 14; however, 9 additional subjects scanned after December 2014 were identified from a review of 125 cases and were included in the study after having been found to meet criteria 2 and 3. Most excluded from the study failed to meet criterion 1. The full population of 23 subjects with clinical presentations of NPH evaluated in this study responded positively to shunt surgery as evaluated by a neurologist (J.G.). Of the 23 patients with hydrocephalus included in the study, 15 demonstrated a risk of hypertension, 7 patients had diabetes, 10 had hyperlipidemia, 3 had coronary artery disease, and 7 tested negative for any cardiovas-

cular risk factors. Ten patients demonstrated comorbidities for ≥2 the risk factors listed above.

Control subjects were recruited retrospectively from the New York University Alzheimer Disease Center to undergo a full clinical research evaluation per Uniform Data Set procedures for Alzheimer Disease Centers,[11] and a brain MR imaging, including high-resolution MPRAGE and the appropriate diffusion MR imaging protocol. Healthy control subjects had no evidence of dementia or mild cognitive impairment and had a Clinical Dementia Rating global score of 0. Subjects with Alzheimer disease were given a diagnosis based on the *Diagnostic and Statistical Manual of Mental Disorders*[12] and the National Institute of Neurological and Communicative Diseases and Stroke/Alzheimer Disease and Related Disorders Association criteria for probable Alzheimer disease[13] and a Clinical Dementia Rating of ≥0.5 (range, 0.5–2.0) and were not deemed to have any medical, neurologic, or psychiatric conditions that could otherwise account for the dementia. The 3 groups did not statistically differ in demographic characteristics (Table 1). Due to the sensitivity of the diffusion MR imaging metrics in general to age,[14] age was included as a covariate in all analyses.

MR Imaging Acquisition and Image Processing
MR images were acquired on a 3T Tim Trio system (Siemens, Erlangen, Germany). Patients with NPH were scanned before ventricular shunt placement. The MR imaging protocol included 3D T1-weighted imaging for anatomic reference using an MPRAGE sequence and diffusion imaging with 3 b-values (0, 1000, 2000 s/mm^2) along 60 diffusion-encoding directions using a single-shot twice-refocused echo-planar sequence. Data were acquired in an 88 × 80 × 30 matrix with 2.6 × 2.6 mm resolution and 5-mm slice thickness. Diffusion-weighted MR images were preprocessed by denoising using a Gaussian smoothing kernel, followed by motion and eddy current correction using the FMRIB Software Library (FSL; http://www.fmrib.ox.ac.uk/fsl) and then the kurtosis tensor was fitted using a constrained weighted linear least-squares fit using in-house software[15] written in Matlab (MathWorks, Natick, Massachusetts). The kurtosis tensors were then used to derive the diffusional kurtosis imaging–acquired parametric maps of mean diffusivity, axial diffusivity (AD), radial diffusivity, fractional anisotropy (FA), mean kurtosis, axial kurtosis (AK), and radial kurtosis. The axonal water fraction (ie, the ratio of intra-axonal water to intra-plus-extra-axonal water) was computed in addition to standard diffusion and kurtosis measures based on a 2-compartment model of neuronal tissue.[7]

Along-Tract Analysis
Tracts were generated using MRtrix (github.com/MRtrix3/mrtrix3) by manually placing seed ROIs in the cerebral peduncles and in the precentral gyrus of each subject. Streamline propagation was constrained using an FA value of 0.2 and a maximum angle of 45°. Streamlines were reoriented to begin at the brain stem and stretch cephalad toward the precentral gyrus. They were then truncated at the middle cerebellar peduncle and pial surface to ensure that tracts from different subjects could be compared without individual anatomy biasing results. To prevent partial volume effects from potentially biasing the analysis, we excluded
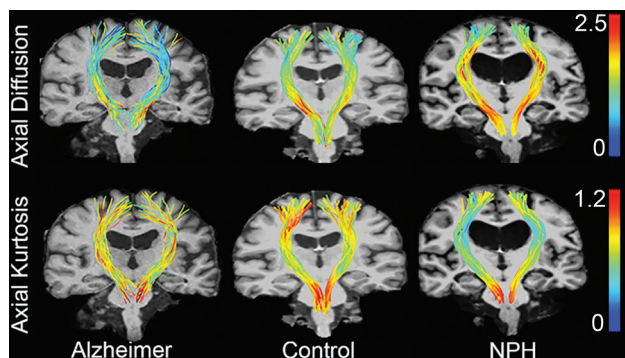
FIG 1. Axial diffusion and axial kurtosis overlaid onto the corticospinal tract as a scalar value and represented by a color: Red indicates higher axial kurtosis or axial diffusivity, while blue indicates lower values. From *left* to *right*, we show sample tracts for patients with Alzheimer disease, healthy controls, and patients with hydrocephalus. Patients with NPH have much lower axial diffusion in periventricular regions than control groups and much greater axial kurtosis values in the same region next to the ventricles.

tracts that came close to or intersected with the lateral ventricles by creating an ROI of the lateral ventricles, dilating it by 1 voxel, and discarding any streamline that intersected this region.

Using Matlab, we normalized tracts using cubic spline interpolation so that the same anatomy occurred at the same distance along the tract for each subject, and vertices were relocated so that there were exactly 100 vertices per streamline along the entire tract, similar to the methods used in Colby et al.[16] The cerebral peduncles were constrained to exist at 25% of the distance from the middle cerebellar peduncle, and the anterior end of the precentral gyrus was constrained to 95%. Parametric diffusion, kurtosis, and white matter tract integrity maps were resampled onto tract vertices as scalar values. Figure 1 provides a qualitative demonstration of axial diffusion and axial kurtosis mapped into the corticospinal tract of a representative sample of a patient with Alzheimer disease, a healthy control, and a patient with hydrocephalus.

Periventricular white matter lesions were segmented for each subject based on T1 hypointensities and FLAIR hyperintensities from FreeSurfer parcellation of T1-weighted MPRAGE images (http://surfer.nmr.mgh.harvard.edu), followed by a nonlinear warp to a common space computed using the FMRIB Nonlinear Registration Tool (FNIRT; http://fsl.fmrib.ox.ac.uk/fsl/fslwiki/FNIRT). These segmentations were used to create leukoaraiosis probability maps to help visualize the location where this pathology is most likely to occur for patients with NPH, patients with Alzheimer disease, and healthy controls and to determine whether leukoaraiosis has a local impact on microstructural pathology associated with NPH.

Statistical Methods

One-way ANCOVA with age as a covariate was used to compare differences between patients with NPH and those with Alzheimer disease, those with NPH and healthy controls, and patients with Alzheimer disease and healthy controls at each point along the CST. A Bonferroni correction for multiple comparisons was used to correct for the presence of the 3 groups. The paired-samples *t* test was used to test for differences across hemispheres. Receiver operating characteristic curves were used to test the diagnostic
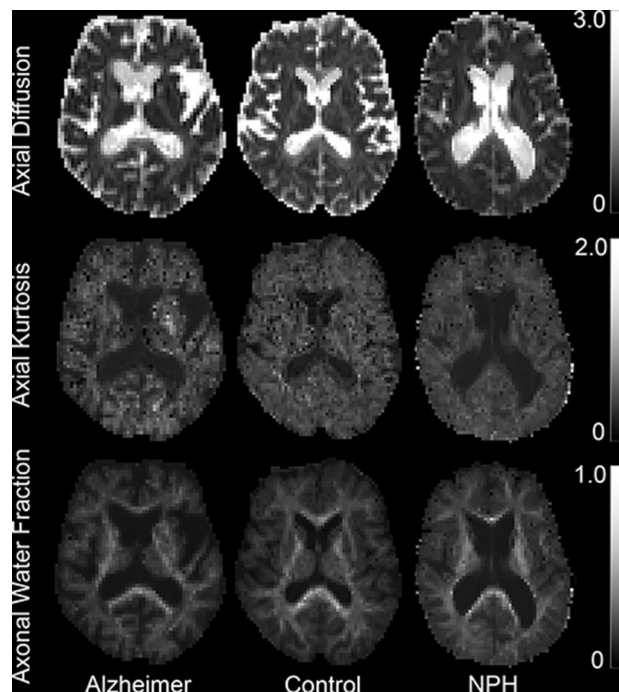

FIG 2. Sample parametric maps for patients with Alzheimer disease, healthy controls, and those with normal pressure hydrocephalus to qualitatively demonstrate values that are being mapped to the CST. From *upper* to *lower*, the maps show values for axial diffusivity, axial kurtosis, and axonal water fraction.

accuracy using the area under the receiver operating characteristic curve (AUC) of each diffusion metric and to determine the ones to best differentiate among study groups. One-way ANCOVA controlling for age was used to test for group differences in periventricular leukoaraiosis.

RESULTS

Along-Tract Analysis

Diffusion and kurtosis measures were computed for each subject and then sampled onto the corticospinal tract. Of all diffusion parameters examined during this study, axial diffusivity, axial kurtosis, and the axonal water fraction were found to differentiate subject groups with the greatest level of accuracy. Figure 2 shows sample parametric maps of AD, AK, and AWF to demonstrate the quality of these parameters. Values along the CST were averaged for each hemisphere separately, and groups were compared at each vertex for each diffusion parameter. Axial diffusivity differs significantly across groups ($P < .05$) between 65% and 85% of the distance along the tract; this area is located superior to the internal capsule but below the cortex. On-line Fig 1 provides a reference image to demonstrate the anatomic location where group differences may occur. Figure 3A plots the axial diffusion as a function of the distance on the tract from the superior end of the brain stem.

Axial kurtosis demonstrates the largest difference among groups both in terms of P values $< .05$ and in the number of significant voxels. Figure 3B shows the change in axial kurtosis, which significantly differs ($P < .05$) between groups from 50% to 90% of the distance along the CST. Figure 3C shows the change in the along-tract AWF, which significantly differs ($P < .05$) across
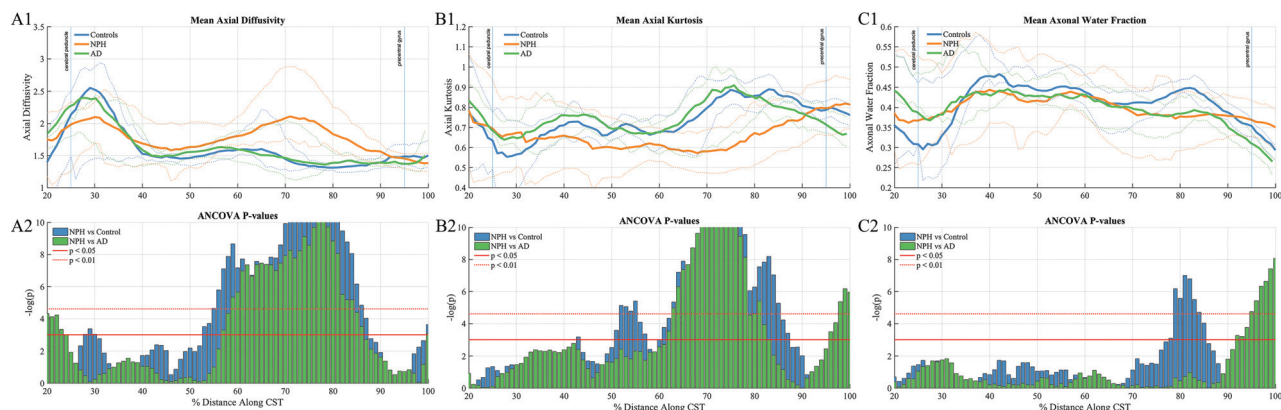
FIG 3. *A*: Along-tract group differences in axial diffusivity among patient groups. *A1*: Axial diffusion at each point along the CST in the right hemisphere. *A2*: ANCOVA *F*-test results show a significant difference between the NPH group and the Alzheimer and control groups at distances between 56% and 88%. *B*: Along-tract group differences in axial kurtosis among patient groups. *B1*: Axial kurtosis at each point along the CST in the right hemisphere. *B2*: ANCOVA *F*-test results show a significant difference between the NPH group and the Alzheimer and control groups at distances between 50% and 90%. *C*: Along-tract group differences in the axonal water fraction among patient groups. *C1*: Axonal water fraction at each point along the CST in the right hemisphere. *C2*: ANCOVA *F*-test results show a significant difference between the NPH group and the Alzheimer and control groups at distances between 67% and 86%.

Table 2: Values measured in the corona radiata, located at 70%–75% of the distance along the CST[a]

	NC (n = 11) (Mean)	Alzheimer Disease (n = 10) (Mean)	NPH (n = 23) (Mean)	NPH vs Alzheimer Disease		NPH vs NC		Alzheimer Disease vs NC	
				P Value	AUC	P Value	AUC	P Value	AUC
FA	0.44 ± 0.07	0.39 ± 0.05	0.51 ± 0.10	0.01[b]	0.88	0.04	0.76	0.12	0.76
MD	0.88 ± 0.05	0.89 ± 0.06	1.30 ± 0.37	0.02[b]	0.87	<0.01[b]	0.94	0.80	0.79
RD	0.67 ± 0.05	0.69 ± 0.07	0.93 ± 0.37	0.18	0.65	0.04[b]	0.76	0.53	0.84
AD	1.30 ± 0.08	1.26 ± 0.07	2.04 ± 0.39	<0.01[c]	0.96	<0.01[c]	1.0	0.60	0.51
MK	1.08 ± 0.09	1.04 ± 0.09	0.99 ± 0.19	0.94	0.52	0.35	0.73	0.66	0.82
RK	1.40 ± 0.14	1.19 ± 0.22	1.54 ± 0.42	0.03	0.82	0.34	0.62	0.10	0.82
AK	0.86 ± 0.07	0.97 ± 0.06	0.63 ± 0.11	<0.01[c]	0.97	<0.01[c]	0.98	0.11	0.67
AWF	0.42 ± 0.02	0.39 ± 0.03	0.38 ± 0.07	0.88	0.66	0.22	0.74	0.12	0.86

Note:—MD indicates mean diffusivity; RD, radial diffusivity; MK, mean kurtosis; RK, radial kurtosis; NC, healthy controls.
[a] Values for the left and right hemispheres did not differ significantly (paired sample *t* test) and were averaged.
[b] $P < .05$.
[c] $P < .01$.

groups in areas correlating with changes that occur in AK (between 67% and 86%).

Table 2 shows the mean and SD for all diffusion parameters analyzed during this study, as well as the results of receiver operating characteristic analysis in the periventricular region and AUC values for each metric at a tract distance of 75%. Seventy-five percent marks the approximate location of the corona radiata in each patient. This region was chosen because it is part of the region with the largest difference among all diffusion parameters among groups. Axial diffusivity showed the highest AUC with a value of 1.0. We also found significant differences between the NPH and Alzheimer groups in FA values, which agree with measurements made in literature.[17] In addition to increased AD and FA in those with NPH compared with control groups, MD was also found to be significantly increased and AK and RK were found to be significantly decreased. AUC values (NPH versus controls) for mean diffusivity, AD, and AK were 0.94, 1.0, and 0.98, respectively, indicating that these parameters had the highest performance in differentiating those with NPH from controls.

Relationship with Leukoaraiosis
The extent of leukoaraiosis was significantly greater in patients with NPH ($P < .05$), with volumes greater than either the Alzheimer group or the healthy control group. Figure 4 provides leukoaraiosis probability maps for each patient group, describing the extent to which leukoaraiosis may be affecting the corticospinal tract.

DISCUSSION
This study measured the microstructural properties of the CST in the 3 patient cohorts; the AUC findings here suggest that AD and AK can be used as markers for a clinical diagnosis of NPH in the presence of a confusing radiologic presentation. We found that pathology in NPH is located in the upper periventricular part of the CST, extending from the superior corona radiata to the posterior internal capsule. The most striking results were found in AD, AK, and AWF parameters. AD values were found to be higher in NPH than in Alzheimer and control groups up to a factor of 2, while AK and AWF were found to be lower by up to 45% and 21%, respectively, in the periventricular regions. The results found here also agree well with the work of other groups who have previously compared kurtosis measurements in white matter between those with NPH and controls. Kamiya et al[17] found that in the internal capsule through the corona radiata regions, FA, mean diffusivity, and AD were significantly increased in those with NPH compared with controls, while mean kurtosis was decreased compared with
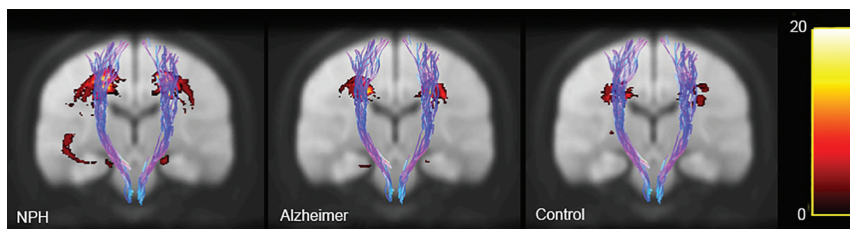
FIG 4. Leukoaraiosis heat maps. Yellow areas show regions where patients are most likely to have leukoaraiosis. Probability maps are shown on top of the 1-mm brain of the Montreal Neurological Institute 152 space.

the control group. We found very similar results for these particular diffusion parameters (Table 2), which helps provide confidence in the accuracy of this analysis.

These measurements have implications for the relative structure of periventricular white matter tract microarchitecture in NPH. Other studies have hypothesized that the white matter in NPH may be compressed due to mechanical pressure caused by ventricular dilation.[18,19] This is consistent with our observation that an increase in axial diffusivity is seen in regions near the ventricle in patients with NPH. In particular, we found group differences in the corona radiata, where though several major white matter tracts are known to cross, evidence of motor neurons responsible for limb control have been identified[19] in addition to motor neurons related to bladder control,[20] both of which are known to become impaired in NPH.

Increased axial diffusivity in patients with hydrocephalus compared with healthy controls and patients with Alzheimer disease implies more diffusion and coherent fiber alignment in the direction parallel to axon orientation, which may mean that NPH causes tracts to be more aligned in regions near the ventricles due to ventricular expansion. Increased diffusion also has the potential to be caused by local edema[21]; however, the indication that it is measuring fiber coherence is supported by increased FA values provided in Table 2. We also saw decreased axial kurtosis in patients with NPH, implying a decrease in microstructural complexity and a decrease in barriers to diffusion in the direction parallel to axonal orientation. Evidence suggests that up to a certain point, white matter changes in NPH are believed to be reversible, but permanent atrophy of the white matter can develop.[22] Decreased axonal water fraction values imply a smaller fraction of axons in each voxel; this means that even though fibers are more tightly aligned in NPH due to ventricular expansion, the packing density of these fibers has decreased. While AWF is significantly decreased in those with NPH compared with controls, it does not differ from that of Alzheimer disease. This may relate to some of the similarities seen between the 2 types of dementia or that atrophy in the region of decreased AWF is related to increased ventricular size. Decreased AWF may imply that mechanical pressure on periventricular axons leads to atrophy and permanent damage to the CST or that these fibers may be decreasing in diameter.

Cerebral white matter changes are associated with aging as well as cerebrovascular risk factors and have a high prevalence in patients with hydrocephalus.[23] In our previous work,[24] we found a strong correlation between the presence of leukoaraiosis and diffusion parameters within ROIs in the internal capsule. Figure 4 quantifies the likelihood of each patient population having leu-

koaraiosis at any location in the brain. It is possible that mechanical stress on the brain is the cause of both changes observed in diffusion measurements as well as the presence of white matter lesions visible in the brains of diseased patient groups. However, our results indicate an independent NPH effect because even when the analysis is limited to where leukoaraiosis is shared (Table 2), we still see a significant difference in diffusion and kurtosis values. This suggests that differences in diffusion and kurtosis measures cannot be due to the presence of leukoaraiosis alone.

In the future, this study should be expanded to include control populations with ventricles with sizes comparable to those in the NPH group. Furthermore, while we hypothesize that ventricular expansion may lead to permanent cell damage in the CST, this is only a possible explanation of our findings. This should be explored in follow-up studies examining postoperative kurtosis in patients who improve following shunt operations. The small size of the Alzheimer disease and healthy control populations potentially limits the reproducibility of this study. Future longitudinal analysis of NPH, AD, and healthy control populations will help provide certainty in the precision of the results presented here.

CONCLUSIONS

The along-tract analysis performed here provides a unique perspective on the localization of pathology in hydrocephalus. Examining the brain along its constituent tracts, rather than simply averaging all the data within them allows a better understanding of the mechanics of deformations occurring in the brain in hydrocephalus.

This study demonstrates that normal pressure hydrocephalus can be characterized by decreased axial kurtosis and increased axial diffusivity as well as a decreased axonal water fraction in the cortical spinal tract. The findings suggest that these measures can be used as diagnostic markers to help differentiate those with NPH and Alzheimer disease and healthy subjects, as reflected by axial kurtosis and diffusivity measures, at a specific periventricular region of the corticospinal tract. Axonal water fraction deficits may reflect microstructural damage. We hope to use these features in isolation and in combination with other distinct features as diagnostic as well as prognostic features of NPH that will help determine patient management in a noninvasive manner.

article. We would also like to thank Jim Babb for his helpful critique of our statistical methods.

REFERENCES

1. Adams RD, Fisher CM, Hakim S, et al. **Symptomatic occult hydrocephalus with "normal" cerebrospinal-fluid pressure: a treatable syndrome.** *N Engl J Med* 1965;273:117–26 CrossRef Medline
2. Tarnaris A, Kitchen ND, Watkins LD. **Noninvasive biomarkers in normal pressure hydrocephalus: evidence for the role of neuroimaging.** *J Neurosurg* 2009;110:837–51 CrossRef Medline
3. Bradley WG. **Normal pressure hydrocephalus: new concepts on etiology and diagnosis.** *AJNR Am J Neuroradiol* 2000;21:1586–90 Medline
4. Jensen JH, Helpern JA. **MRI quantification of non-Gaussian water diffusion by kurtosis analysis.** *NMR Biomed* 2010;23:698–710 CrossRef Medline
5. Jensen JH, Helpern JA, Ramani A, et al. **Diffusional kurtosis imaging: the quantification of non-gaussian water diffusion by means of magnetic resonance imaging.** *Magn Reson Med* 2005;53:1432–40 CrossRef Medline
6. Fieremans E, Jensen JH, Helpern JA. **White matter characterization with diffusional kurtosis imaging.** *Neuroimage* 2011;58:177–88 CrossRef Medline
7. Fieremans E, Benitez A, Jensen JH, et al. **Novel white matter tract integrity metrics sensitive to Alzheimer disease progression.** *AJNR Am J Neuroradiol* 2013;34:2105–12 CrossRef Medline
8. Jelescu IO, Zurek M, Winters KV, et al. **In vivo quantification of demyelination and recovery using compartment-specific diffusion MRI metrics validated by electron microscopy.** *Neuroimage* 2016;132:104–14 CrossRef Medline
9. Benitez A, Fieremans E, Jensen JH, et al. **White matter tract integrity metrics reflect the vulnerability of late-myelinating tracts in Alzheimer's disease.** *Neuroimage Clin* 2014;4:64–71 CrossRef Medline
10. Golomb J, Wisoff J, Miller DC, et al. **Alzheimer's disease comorbidity in normal pressure hydrocephalus: prevalence and shunt response.** *J Neurol Neurosurg Psychiatry* 2000;68:778–81 CrossRef Medline
11. Morris JC, Weintraub S, Chui HC, et al. **The Uniform Data Set (UDS): clinical and cognitive variables and descriptive data from Alzheimer Disease Centers.** *Alzheimer Dis Assoc Disord* 2006;20:2101–06 CrossRef Medline
12. Gmitrowicz A, Kucharska A. **Developmental disorders in the fourth edition of the American classification: Diagnostic and Statistical Manual of Mental Disorders (DSM IV: optional book)** [in Polish]. *Psychiatr Pol* 1994;28:509–21 Medline
13. McKhann G, Drachman D, Folstein M, et al. **Clinical diagnosis of Alzheimer's disease: report of the NINCDS-ADRDA Work Group under the auspices of Department of Health and Human Services Task Force on Alzheimer's Disease.** *Neurology* 1984;34:939–44 CrossRef Medline
14. Sullivan EV, Pfefferbaum A. **Diffusion tensor imaging and aging.** *Neurosci Biobehav Rev* 2006;30:749–61 CrossRef Medline
15. Veraart J, Rajan J, Peeters RR, et al. **Comprehensive framework for accurate diffusion MRI parameter estimation.** *Magn Reson Med* 2013;70:972–84 CrossRef Medline
16. Colby JB, Soderberg L, Lebel C, et al. **Along-tract statistics allow for enhanced tractography analysis.** *Neuroimage* 2012;59:3227–42 CrossRef Medline
17. Kamiya K, Kamagata K, Miyajima M, et al. **Diffusional kurtosis imaging in idiopathic normal pressure hydrocephalus: correlation with severity of cognitive impairment.** *Magn Reson Med Sci* 2016;15:316–23 CrossRef Medline
18. Nakanishi A, Fukunaga I, Hori M, et al. **Microstructural changes of the corticospinal tract in idiopathic normal pressure hydrocephalus: a comparison of diffusion tensor and diffusional kurtosis imaging.** *Neuroradiology* 2013;55:971–76 CrossRef Medline
19. Kim JS, Pope A. **Somatotopically located motor fibers in corona radiata: evidence from subcortical small infarcts.** *Neurology* 2005;64:1438–40 CrossRef Medline
20. Sakakibara R, Panicker J, Fowler CJ, et al. **Vascular incontinence: incontinence in the elderly due to ischemic white matter changes.** *Neurol Int* 2012;4:e13 CrossRef Medline
21. Ebisu T, Naruse S, Horikawa Y, et al. **Discrimination between different types of white matter edema with diffusion-weighted MR imaging.** *J Magn Reson Imaging* 1993;3:863–68 CrossRef Medline
22. Del Bigio MR. **Cellular damage and prevention in childhood hydrocephalus.** *Brain Pathol* 2004;14:317–24 Medline
23. Pantoni L, Garcia JH. **Pathogenesis of leukoaraiosis: a review.** *Stroke* 1997;28:652–59 CrossRef Medline
24. Serulle Y, Pawar RV, Eubig J, et al. **Diffusional kurtosis imaging in hydrocephalus.** *Magn Reson Imaging* 2015;33:531–36 CrossRef Medline
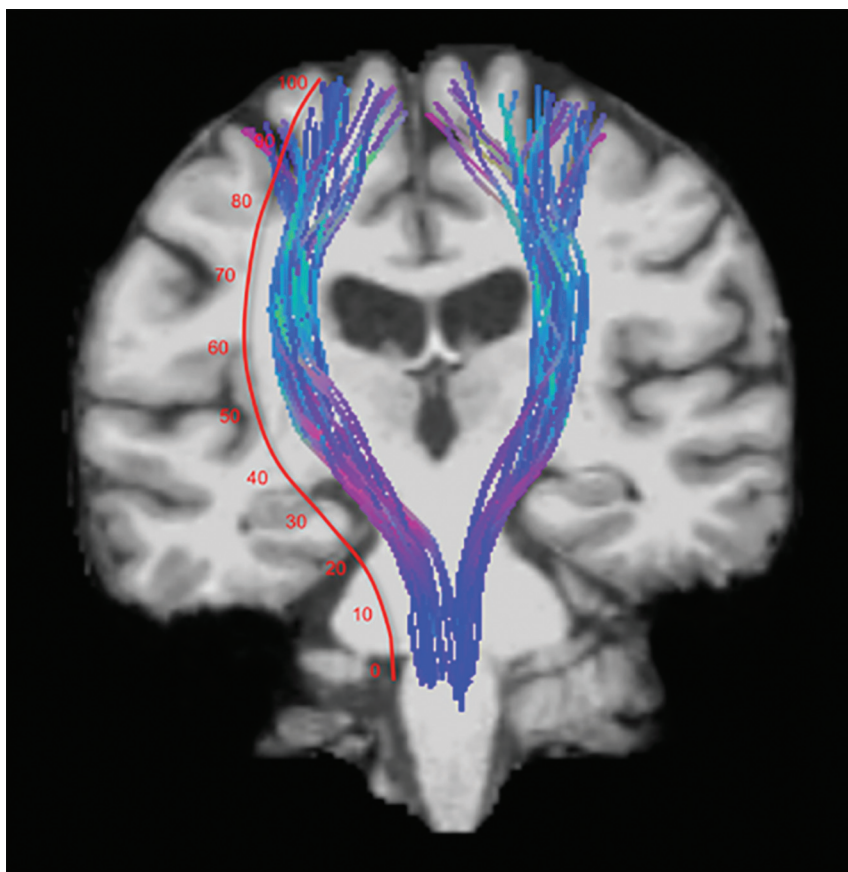
ON-LINE FIGURE. Demonstration of anatomy as a function of the percentage distance along the corticospinal tract. This image can be used as a reference so that readers can visualize the anatomy where group differences occur.